Flicker emission of wind farms during continuous operation

Joaquín Mur-Amada, Ángel A. Bayod-Rújula

Zaragoza University, Department of Electrical Engineering
C/ María de Luna 3, Ed. Torres Quevedo
50018 – Zaragoza (Spain)
phone: +34 976 761920, e-mail: joako@unizar.es and aabayod@unizar.es

***Abstract*— Flicker emission of a wind farm during continuous operation has three main sources: wind turbulence, tower shadow and generator or power converter oscillations at frequencies near 8,8 Hz. Flicker emission of a wind farm during continuous operation can be derived from the output of a single wind turbine since fast fluctuations are low correlated among turbines. A stochastic model of the power spectral density (PSD) of power output is parameterized and a simple formula is derived to estimate flicker level from PSD and network parameters. This simple formula assesses the individual influence in flicker level of wind turbulence, tower shadow and generator/converter.**

The model has been tested with data from several wind farms. In wind farms with induction generators and squirrel cage or variable resistance rotor, wind turbulence was the main flicker source since the turbine coupling was soft enough to damper generator oscillations and torque variations related to rotor angle. In wind farms with doubly fed induction generators, the main flicker source was the induced noise at frequencies around maximum flicker sensitivity by the power converter. In the cases analyzed, the flicker level was very low due to the strength of the network at the point of common coupling.

***Index Terms*—wind power, flicker, stochastic process.**

List of acronyms

DFIG Doubly Fed Induction Generator
PCC Point of Common Coupling
PSD Power Spectral Density
P_{st} Short Time Flicker Emission Level
RMS Root Mean Squared (value or error)
SQIG Squirrel Cage Induction Generation
VRIG Variable Resistance Induction Generator

I. Introduction

This work is based on the literature review in [1] of wind turbine power output PSD [2] and the stochastic analysis in [3] of tower shadow inside a wind farm. The instantaneous output of a wind farm can be expressed in the frequency domain using phasors:

$$P_{farm}(t) = \mathrm{Re}\left[\int_0^\infty \vec{S}_{farm}(f)\, e^{j2\pi f\, t} df\right] \quad (1)$$

where j is the imaginary unit, complex variables are denoted by an arrow and Re states for the real part of a complex number. Neglecting farm grid losses, the complex sum of the frequency components of each turbine $\vec{S}_{turbine\ i}(f)$ totals the approximate farm output, $\vec{S}_{farm}(f)$.

$$\vec{S}_{farm}(f) = S_{farm}(f)\, e^{j\varphi_{farm}(f)} \approx \sum_{i=1}^{N_{turbines}} S_{turbine\ i}(f)\, e^{j\varphi_i(f)} \quad (2)$$

Fast fluctuations of the turbines have low spatial correlation [4, 5] and wind gusts have frequencies with low flicker sensitivity. In fact, the coherence for the usual dimensions of wind farms is low at frequencies above 1 mHz [6]. In [7], the correlated component of wind is estimated from the Davenport type and Schlez and Infield's decay factors [8], showing that coherence for distances greater than 100 m is negligible at frequencies f >0,5 Hz.

Experimental measurements [9] have shown that the synchronisation of the turbine blades passing the tower is unlikely. According to [10], a very steady wind, very uniformly distributed and a weak electrical network is necessary for synchronisation to happen driven by voltage dips. Moreover, simultaneous tower shadow at all turbines in a wind farm is a very uncommon event whose probability is stated in [3].

II. Estimation of Voltage Fluctuations

According to [3], the fluctuations in the range of flicker sensitivity can be modeled as stochastically independent processes. Tower shadow fluctuations depend on the turbine blade position. Since there is no explicit time origin, fluctuations can happen at any time with the same probability. The phase differences among turbine blades i and j is $\varphi_{i,j}$ and they are uniformly distributed in $[-\pi, +\pi]$. Thus, the spectrum phase does not contain stochastically relevant information.

Periodic fluctuations (usually related to rotor angle) appear as peaks at their frequency in the spectrum, whereas fluctuations such as turbulence, which have neither a periodic pattern nor a characteristic frequency, can be associated with the tendency of the periodogram [1].

A. Characterization of PSD of the Farm Power Output

The tower shadow shape in various turbines has been measured by the authors in [9]. Fig. 1 shows the typical behavior of a 750 kW wind turbine (squirrel cage induction generator and stall regulation) for wind speeds around 6,5 m/s. The tower shadow amplitude is around $P_0 / 30$ with some low-frequency amplitude modulation. For simplicity, tower shadow of Fig. 1 can be characterized as a

sinusoidal fluctuation at the blade frequency with randomly modulated amplitude [11]. In Fig. 2 and Fig. 3, the original power spectrum is in grey whereas the averaged periodogram $\langle {S_{farm}}^2(f) \rangle$ is the thin black line (the notation $\langle x \rangle$ stands for average or expected values of the random quantity x).

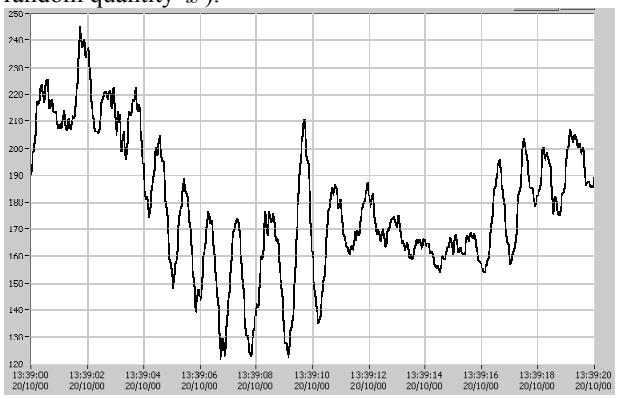

Fig. 1: Active power of a NTM 750 kW wind turbine for wind speeds around 6,5 m/s.

The power spectrum of the farm power output is the modulus of a random phasor ${S_{farm}}^2(f)$ that varies in time since wind is stochastic (${S_{farm}}^2(f)$ is the grey lines in Fig. 2 and Fig. 3). However, its average, $\langle {S_{farm}}^2(f) \rangle$, is approximately constant for certain operational conditions (see black thin line in Fig. 2 and Fig. 3).

The fluctuation of power output of the farm is the sum of contributions of many turbines (2), which are mainly uncorrelated at the frequencies of interest for flicker analysis. The sum of N independent phasors of random angle of N turbines in the farm $\vec{S}_{farm}(f)$ asymptotically converges to a complex Gaussian distribution of null mean and standard deviation $\sigma_{farm}(f) = \sqrt{N}\sigma_1(f)$, where $\sigma_1(f)$ is the mean RMS fluctuation at a single turbine at frequency f. To be precise, the variance ${\sigma_1}^2(f)$ is half the mean squared fluctuation amplitude at frequency f, $\left\langle \frac{1}{2} \left| \vec{S}_{turbine\ i}(f) \right|^2 \right\rangle$.

In Fig. 2, the PSD shows a wide peak at blade frequency due to the varying amplitude and frequency with harmonics and sub-harmonics. Their effect on flicker depends on the product of sensitivity of flicker to that frequency $\left| F_{weight}(f) \right|$ defined in [13], times the power content of the frequency range (i.e., product of the width by the amplitude of the peak).

Red thick line is the output of a system of fractional order with a root and a pole excited by white noise. Light green dotted line is a measure of the accumulated error of the model integrated from frequency f up to 25 Hz. PSD units are RMS W^2 per hertz (i.e., $\frac{1}{2}\left| \vec{S}_{farm}(f) \right|^2$).

According to [1], the PSD can be approximated by the spectrum of a system of fractional order r ($1 \le r \le 1,6$), plus the tower shadow effect S_0 (a delta impulse δ_0 at frequency f_0) and the noise floor S_2. In the frequencies of interest for flicker analysis, $0,05\ Hz < f \le 35\ Hz$, the following approximations are valid:

$$\left\langle {S_{farm}}^2(f) \right\rangle \approx N\, S_1 \left(S_0\, \delta_0(f - f_0) + f^{-2r} + S_2 \right) \qquad (3)$$

$$\sigma_{farm}{}^2(f) = \tfrac{1}{2} \left\langle {S_{farm}}^2(f) \right\rangle \qquad (4)$$

$$\vec{S}_{farm}(f) \sim \mathbb{C}N\left[0, \sigma_{farm}(f)\right] \qquad (5)$$

$$S_{farm}(f) \sim Rayleigh\left[\sigma_{farm}(f)\right] \qquad (6)$$

$$\left| \vec{S}_{farm}(f) \right|^2 \sim Exponential\left[\tfrac{1}{2}{\sigma_{farm}}^{-2}(f)\right] \qquad (7)$$

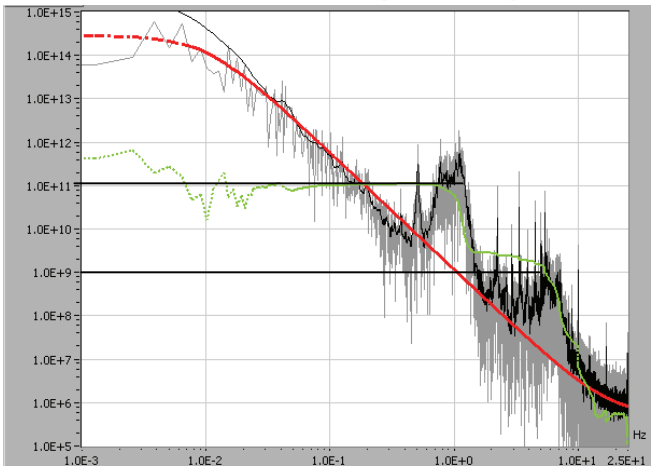

Fig. 2: PSD of active power of a NTM 750 kW wind turbine for wind speeds around 6,5 m/s.

Table I: Parameters of the PSD model of active power turbine output (4)

	Significance	Range
r	System order of the turbine active power output excited by the wind turbulence (i.e., half the slope trend of PSD in a double logarithmic plot)	1 ~ 1.7
$\frac{S_1}{{S_n}^2}$	Overall fluctuation level of the turbine (i.e., the PSD trend line at 1 Hz) in p.u. units	10^{-4}~10^{-2}
S_0	Squared average of tower shadow power oscillation relative to S_1	5~100
f_0	Mean tower shadow frequency	0.5~2 Hz
S_2	Squared noise level on power output relative to S_1	0~0.01
S_n	Nominal power of the turbine	0,3~5 MW
N	Number of equivalent turbines in the farm	1~50

Parameters r, f_0, S_1 and S_2 can be estimated from PSD by regression analysis. Notice that in general, harmonic peaks are narrow and their power content is low. Sub-harmonics can have noticeable power, but their flicker sensitivity is low. These terms can be added explicitly to (3) as delta impulses. Nevertheless, models more complex than (3) are also suitable. For simplicity, S_0 can include also the effect of tower harmonics and sub-harmonics:

$$S_0 = \int_{0,05Hz}^{8,8Hz} \left(\frac{1}{S_1} \left\langle {S_{farm}}^2(f) \right\rangle - f^{-2r} - S_2 \right) \frac{\left| F_{weight}(f) \right|^2}{\left| F_{weight}(f_0) \right|^2} df \approx$$

$$\approx \int_{0,05Hz}^{8,8Hz} \left(\frac{1}{S_1} \left\langle {S_{farm}}^2(f) \right\rangle - f^{-2r} - S_2 \right) \frac{f^2}{{f_0}^2} df \qquad (8)$$

If PSD does not fit the model (3) at frequencies between 8,8 Hz and 35 Hz, another delta impulse term S_3 at frequency 8,8 Hz < f_3 < 35 Hz can be included in (3):

$$S_3 = \int_{8,8Hz}^{35Hz} \left(\frac{1}{S_1} \left\langle {S_{farm}}^2(f) \right\rangle - f^{-2r} - S_2 \right) \frac{\left|F_{weight}(f)\right|^2}{\left|F_{weight}(f_3)\right|^2} df S_3 \approx$$

$$\approx \int_{8,8Hz}^{35Hz} \left(\frac{1}{S_1} \left\langle {S_{farm}}^2(f) \right\rangle - f^{-2r} - S_2 \right) \frac{f^{-3}}{{f_3}^{-3}} df \qquad (9)$$

Approximations (8) or (9) assume no correlation of fluctuations included in terms S_0 or S_3. If this assumption does not hold, formulas must be modified accordingly.

These formula indicate that the relative importance of fluctuations is proportional to f^2 up to 8,8 Hz and then proportional to f^{-3}.

Spectrum angle $\varphi_{farm}(f)$ is a random variable uniformly distributed in $[-\pi, +\pi]$. Consequently, the complex phasor $\vec{S}_{farm}(f)$ is a complex Gaussian random variable of zero mean and standard deviation $\sigma_{farm}(f)$:

$$\vec{S}_{farm}(f) \sim \mathbb{C}N\left[0, \sigma_{farm}(f)\right] \qquad (10)$$

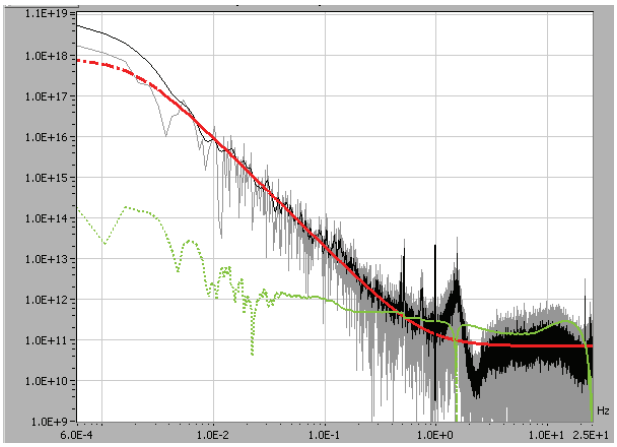

Fig. 3: PSD of a DFIG wind farm operating at low winds.

B. Contribution of power fluctuations to Flicker

1) Voltage variations of induced by power fluctuations

The approach followed in this section is based in [12], where a simplified model of the wind farm is derived based on the fourth-pole equivalent representation of the electrical elements, the distributed layout of the turbines, the stochastic nature of power output and small-signal analysis of the grid.

The approximated voltage variation can be obtained from the linear model of circuit in Fig. 4:

$$\Delta U \underset{approx}{\simeq} \langle \Delta U \rangle + \frac{R_{fic} \cdot \Delta P + X_{fic} \cdot \Delta Q}{U_{PCC}} \qquad (11)$$

where ΔP and ΔQ are the active and reactive power deviation from their average of the wind farm at the point of common coupling with the grid (PCC), U_n is the nominal voltage at PCC, R_{fic} and X_{fic} are the equivalent resistance and reactance at PCC.

Usually, fluctuations involved in flicker phenomena are slow enough for neglecting dynamics of generators. Therefore, in most situations, the static P vs Q curves are suitable to account dependence of active and reactive power.

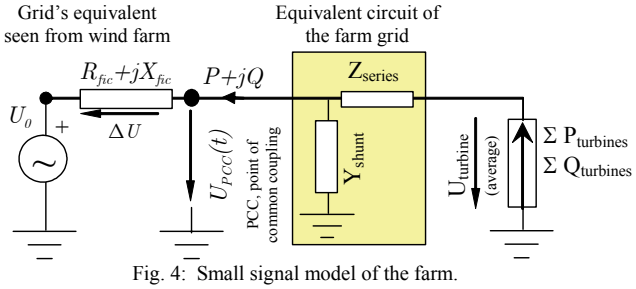

Fig. 4: Small signal model of the farm.

Assuming that ΔP and ΔQ are linearly correlated at PCC given some operational conditions, the marginal voltage-current lag angle $\varphi = \arctan(\Delta Q / \Delta P)$ is approximately constant, then voltage deviations are proportional to power deviations: (12)

$$\Delta U \simeq \langle \Delta U \rangle + \frac{R_{fic} + X_{fic} \tan(\varphi)}{U_{PCC}} \Delta P = \langle \Delta U \rangle + \beta U_{PCC} \Delta P$$

where β is a sensitivity coefficient of voltage to power fluctuations. β can be expressed in terms of apparent short-circuit power $S_{k,fic}$, its network impedance angle ψ_k and voltage-current lag angle φ. β usually ranges from 0.1 to 0.005 p.u.

$$\beta = \frac{R_{fic} + X_{fic} \tan(\varphi)}{{U_{PCC}}^2} = \frac{\cos(\psi_k) + \sin(\psi_k) \tan(\varphi)}{S_{k,fic}} \qquad (13)$$

Thus, the voltage at the PPC of the farm can be expressed with random phasors, according to Fig. 4:

$$U_{PCC}(t) = U_0 + \Delta U \simeq U_0 + \left\langle \Delta U \right\rangle + \beta U_{PCC} \Delta P(t) = \qquad (14)$$
$$= \langle U_{PCC} \rangle - \beta U_{PCC} \operatorname{Re}\left[\int_0^\infty \vec{S}_{farm}(f)\, e^{j2\pi f t} df \right]$$

where $\langle U_{PCC} \rangle$ is the average voltage for a given operational condition. In fact, (14) is the small signal model for voltage respect its mean value $\langle U_{PCC} \rangle$. The parameters U_0, $\langle U_{PCC} \rangle$ and β are actually random variables which depend on nearby loads, generators and grid configuration.

2) Flickermeter functional blocks

According to IEC 61000-4-15 [13], the flickermeter is divided into functional blocks (see Fig. 5). The first block is a normalizing voltage adaptor with proportional constant $1/\langle U_{PCC} \rangle$. The output of the first block is a signal proportional to voltage and unity mean (i.e., per unit voltage respect its average).

$$U_{pu}(t) = 1 + \beta \operatorname{Re}\left[\int_0^\infty \vec{S}_{farm}(f)\, e^{j2\pi f t} df \right] \qquad (15)$$

The output of the quadratic demodulator (block 2) is:

$$U_{pu}{}^2(t) = a(t) = 1 + 2\beta \operatorname{Re}\left[\int_0^\infty \vec{S}_{farm}(f)\, e^{j2\pi f t} df \right] +$$
$$+ \left(\beta \operatorname{Re}\left[\int_0^\infty \vec{S}_{farm}(f)\, e^{j2\pi f t} df \right] \right)^2 \qquad (16)$$

The last term in (16) can be neglected since $\Delta U \ll U$, resulting in the linear relationship $U_{pu}{}^2(t) \approx 2 U_{pu}(t) - 1$. The linear approximation of (16) is implicit when standard IEC61400-21 states that flicker level is proportional to the

short-circuit impedance at PCC or when it recommends the high ratio $S_{k,fic}/S_n \geq 50$. The relationship between the output of block 2 in the time domain $a(t)$ and in the frequency domain $\vec{a}(f)$ is:

$$a(t) = 1 + \mathrm{Re}\left[\int_0^\infty \vec{a}(f)\, e^{j2\pi f\, t} df\right] \quad (17)$$

Assuming linearization in (16), the output of block 2 at frequency f will be a complex normal random phasor with zero mean:

$$\vec{a}(f) \sim \mathbb{C}N\left(0,\, 2\beta\, \sigma_{farm}(f)\right) \quad (18)$$

The weighting filters, named block 3 in IEC 61000-4-15, is equivalent to the multiplication of Fourier components by the filter transfer function. $F_{weight}(f)$ is the weighting transfer function defined in [13] between 0,05 Hz and 35 Hz and zero elsewhere (ideal pass-band sinc filter). Recall that the pass-band filter removes the DC component of the signal $b(t)$.

The phase displacement introduced by a filter in a stochastic signal with circular symmetry does not alter its statistical properties since the phase of the signals is uniformly distributed [14]. Therefore, the standard deviation is multiplied by the filter function modulus $\left|F_{weight}(f)\right|$:

$$\sigma_{\vec{b}}(f) = 2\beta\, \sigma_{farm}(f)\left|F_{weight}(f)\right| \quad (19)$$

The sum (integration) of the projection of phasors $\vec{b}(f)$ in the real axis is $b(t)$. Phasor $\vec{b}(f)$ is a complex normal random variable with zero mean and standard deviation $\sigma_{\vec{b}}(f)$, independently distributed at each frequency f. Therefore $b(t)$ is a real normal random variable of zero mean and standard deviation σ_b, i.e. $b(t) \sim N\left(0,\, \sigma_b\right)$.

$$\sigma_b{}^2 = \int_{0{,}05\,\mathrm{Hz}}^{35\,\mathrm{Hz}} \sigma_{\vec{b}}{}^2(f)\, df \quad (20)$$

The fourth block is another quadratic multiplier. Its output in the time domain is $c(t) = b^2(t) \sim Gamma\left[\frac{1}{2}, 2\sigma_b^2\right]$. Thus, its mean value is $\langle c(t)\rangle = \mu_c = \sigma_b{}^2$ and its standard deviation of $c(t)$ is $\sigma_c = \sqrt{2}\,\sigma_b{}^2$. The average of $c(t)$ can alternatively be computed using Parseval's theorem:

$$\langle c(t)\rangle = \left\langle b^2(t)\right\rangle = \underset{Parseval}{=} \left\langle \frac{1}{2}\int_{0{,}05\,\mathrm{Hz}}^{35\,\mathrm{Hz}} \left|\vec{b}(f)\right|^2 df \right\rangle \quad (21)$$

The modulus of phasor $\vec{b}(f)$ is Rayleigh distributed and its squared modulus is distributed exponentially. Integral (21) can be computed since integration and averaging are interchangeable:

$$\langle c(t)\rangle = \frac{1}{2}\int_{0{,}05\,\mathrm{Hz}}^{35\,\mathrm{Hz}} 2\sigma_{\vec{b}}{}^2(f)\, df = \sigma_b{}^2 \quad (22)$$

In the frequency domain, $\sigma_{\vec{c}}(f)$ can be computed through convolution (in this case the linear approximation applied in (16) is not valid).

$$\vec{c}(f) = \int_{\min(35\,\mathrm{Hz};\, f-0{,}05)}^{\min(35,\max(0{,}05;\, f-35))} \vec{b}(f')\, \vec{b}(f-f')\, df' \quad (23)$$

Phasor $\vec{c}(f)$ is the sum of infinitesimal product terms that are stochastically independent. Thus, the statistical properties of $\vec{c}(f)$ depend on the distribution of $\vec{b}(f')\, \vec{b}(f-f')$. The product of two independent complex normal variables with zero mean and variances $\sigma_{\vec{b}}{}^2(f')$ and $\sigma_{\vec{b}}{}^2(f-f')$ is another random variable with circular symmetry and its modulus distributed as a double-Rayleigh distribution [15]. The average and variance of the modulus of the product of the Fourier coefficients are:

$$\left\langle \left|\vec{b}(f')\, \vec{b}(f-f')\right| \right\rangle = \frac{\pi}{2}\sigma_{\vec{b}}(f')\, \sigma_{\vec{b}}(f-f') \qquad (f' \neq f/2) \quad (24)$$

$$\left\langle \left|\vec{b}(f')\, \vec{b}(f-f')\right|^2 \right\rangle = 4\,\sigma_{\vec{b}}{}^2(f')\,\sigma_{\vec{b}}{}^2(f-f') \qquad (f' \neq f/2) \quad (25)$$

If $f' = f/2$, then the product is distributed exponentially:

$$\left|\vec{b}(f')\, \vec{b}(f-f')\right| = \left|\vec{b}^2(f')\right| \sim Exponential\left[\frac{1}{2\sigma_b{}^2(f/2)}\right] \quad (26)$$

The average of the convolution is null since the integrand $\vec{b}(f')\, \vec{b}(f-f')$ has zero mean (it has circular symmetry). The variance of the convolution is the integration of the variance of the integrand $\vec{b}(f')\, \vec{b}(f-f')$.

$$Var\left[\vec{b}(f')\, \vec{b}(f-f')\right] = 4\,\sigma_{\vec{b}}{}^2(f')\,\sigma_{\vec{b}}{}^2(f-f') \qquad \forall f,\, \forall f' \quad (27)$$

Thus, the variance of phasor $\vec{c}(f)$, $\sigma_{\vec{c}}{}^2(f)$, is:

$$\sigma_{\vec{c}}{}^2(f) = \int_{\min(35\,\mathrm{Hz};\, f-0{,}05)}^{\min(35,\max(0{,}05;\, f-35))} 4\sigma_{\vec{b}}{}^2(f')\, \sigma_{\vec{b}}{}^2(f-f')\, df' \quad (28)$$

If $0{,}1\,\mathrm{Hz} \leq f \leq 70\,\mathrm{Hz}$, then $\vec{c}(f)$ is not null. A Monte-Carlo analysis has shown that $\vec{c}(f)$ is approximately normally distributed, i.e. $\vec{c}(f) \sim \mathbb{C}N\left(0,\, \sigma_{\vec{c}}(f)\right)$. The value of $\sigma_{\vec{c}}{}^2(f)$ can be computed by integration:

$$\begin{aligned}\sigma_{\vec{c}}{}^2(f) = {} & 2^4\beta^4 N^2 S_1{}^2 \Big\{ S_0{}^2 \left|F_{weight}{}^4(f_0)\right| \delta_0(f-2f_0) + \\ & + S_0 \left|F_{weight}{}^2(f_0)\right| \left|F_{weight}{}^2(f-f_0)\right| \Big[\left(f-f_0\right)^{-2r} + S_2\Big] + \\ & 2\int_{\max(0{,}05;\, f-35)}^{f/2} \Big[(f\text{-}f_1)^{-2r} + S_2\Big]\Big[f_1^{-2r} + S_2\Big] \left|F_{weight}{}^2(f\text{-}f_1)\right| \left|F_{weight}{}^2(f_1)\right| df_1 \Big\}\end{aligned} \quad (29)$$

where the integral is computed in half the domain since self convolution has mirror symmetry about $f/2$. Tower shadow contribution to $\sigma_{\vec{c}}{}^2(f)$ is the term in (29) multiplied by $S_0{}^2$ at twice the original frequency. Wind turbulence contribution is the integral term. The cross term of turbulence and tower shadow is the term multiplied by S_0.

After performing the squaring, a first order displacement filter $F_{smooth}(f)$ is applied for obtaining the instantaneous flicker. Notice that the low pass smoothing filter does neither alter the DC value of the signal, $\mu_{flick} = \langle flick(t)\rangle = \langle c(t)\rangle$ nor affect the circular symmetry. A regression formula with 3,5% RMS error is:

$$\begin{aligned}\mu_{flick} = \sigma_b{}^2 \approx {} & \beta^2 N\, S_1 \Big\{ 0{,}0521\, S_0\, f_0{}^{1{,}55} + \\ & + 19{,}02\, S_2 + \tfrac{1}{4}\, Cosh\left[\frac{(r-5{,}383)(r+12{,}548)}{22{,}413}\right]\Big\}\end{aligned} \quad (30)$$

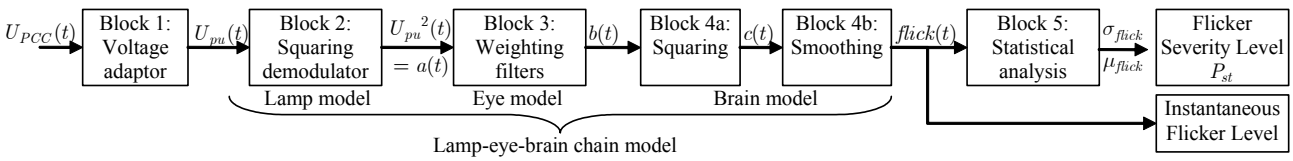

Fig. 5: Simplified block diagram of IEC Flickermeter according to IEC 61000-4-15

μ_{flick} is due to the tower shadow (term multiplied by $S_0\, f_0^2$), the noise floor (term multiplied by S_2), and the turbulence (term of hyperbolic cosine). The three terms are of the same order.

The numeric computation of $\sigma_{\overline{flick}}(f)$ involves three convolutions: $\sigma_{\overline{flick}}{}^2 = \sigma_{\bar{b}}{}^2 * \sigma_{\bar{b}}{}^2 * F_{smooth}{}^2$ and the computation of $\sigma_{flick}{}^2$ requires additional integration (31), resulting in a lengthy process.

$$\sigma_{flick}{}^2 = \int_{0,10\,\mathrm{Hz}}^{70\,\mathrm{Hz}} \sigma_{\overline{flick}}{}^2(f)\, df = \int_{0,10}^{70} \sigma_{\bar{c}}{}^2(f)\, |F_{smooth}(f)|^2 df \qquad (31)$$

Since $|F_{smooth}(f)|^2$ drops quickly to zero, the phasors $\vec{S}_{farm}(f)$ with $f > 2\,\mathrm{Hz}$, and hence, S_2 can be neglected in $\sigma_{flick}{}^2$. A regression formula with 1,4% RMS error is:

$$\sigma_{flick}{}^2 \approx \beta^4 N^2 S_1{}^2 \left[G_1(S_0, f_0) + G_2(r) + G_3(f_0, r) \sqrt{G_1(S_0, f_0) G_2(r)} \right] \qquad (32)$$

where $G_1(S_0, f_0)$ is the term due to tower shadow, $G_2(r)$ is the term due to wind turbulence and $G_3(f_0, r)$ is the cross term.

$$G_1(S_0, f_0) \approx \frac{S_0{}^2 f_0{}^2}{994,72\left(1 - 0{,}2372 f_0 + 0{,}0704 f_0{}^2\right)} \qquad (33)$$

$$G_2(r) \approx \frac{1}{170} + \frac{Exp(0{,}324r + 0{,}1044r^2)}{20710} \qquad (34)$$

$$G_3(f_0, r) \approx 2\,(1 - 0{,}274 f_0)\,(1 - 0{,}1\, r) \qquad (35)$$

In most cases, the main contribution to σ_{flick} is $G_1(S_0, f_0)$ due to the fundamental component of tower shadow and its sub-harmonics.

3) Stochastic characterization of instantaneous flicker

The percentiles of the instantaneous flicker in the statistical classifier of block 5 can be computed assuming some distribution. Since $\mu_{flick}/\sigma_{flick} > 3$ and $\left\langle \mu_{flick}/\sigma_{flick} \right\rangle = 22{,}7$, the flicker level P_{st} depends mainly of mean value of $flick(t)$, μ_{flick}, and only slightly on the statistical distribution of $flick(t)$.

A Monte-Carlo test has been performed for the typical parameter values and the difference between real distribution and Normal distribution is bellow 1% even in the worst case. On average, P_{st} computed from Monte-Carlo is only 0,1% greater than Normal distribution. Assuming normal distribution of the instantaneous flicker $flick(t)$, the short-time flicker P_{st} can be computed algebraically from μ_{flick} and σ_{flick}:

$$P_{st}\,|_{Normal} = \sqrt{0{,}5096\ \mu_{flick} + 0{,}6879\ \sigma_{flick}} \qquad (36)$$

For usual parameter ranges $0{,}72 \le P_{st}/\sqrt{\mu_{flick}} \le 0{,}75$ and a rough estimate of P_{st} is $P_{st} \approx 0.73\sqrt{\mu_{flick}}$ with a 4% RMS error.

III. Parametric Model of Flicker Emission

The relationship of flicker level P_{st} with wind farm parameters has been tracked along flickermeter blocks and it can be computed from (30), (32) and (36). The sensitivity of P_{st} to PSD parameters S_0, f_0, S_2 and r is complex and it can be summarized in (37).

$$P_{st} = \beta \sqrt{N\, S_1 Coef(S_0, f_0, S_2, r)} \qquad (37)$$

β is the flicker sensitivity coefficient at PCC defined in (13) and β usually ranges from 0.1 to 0.005 p.u. Thus:

$$P_{st} = \frac{\cos(\psi_k) + \sin(\psi_k)\tan(\varphi)}{S_{k\ fict}} \sqrt{S_1 N Coef(S_0, f_0, S_2, r)} \qquad (38)$$

where:

$$Coef(S_0, f_0, S_2, r) \approx \frac{0{,}5096\ \mu_{flick} + 0{,}6879\ \sigma_{flick}}{\beta^2 N\, S_1} \qquad (39)$$

r, S_0, f_0, S_1 and S_2 are defined in Table I.

N = number of equivalent turbines in the wind farm.

$S_{k,fic}$ = apparent short-circuit power at PCC

ψ_k = short-circuit angle at PCC

$\tan(\varphi) = \Delta Q / \Delta P$ = average ratio of fluctuations of reactive and active power.

$Coef(S_0, f_0, S_2, r)$ is usually between 0,3 and 1,5 and $\sqrt{S_1 N}/S_k \ll 1$. Thus, the flicker emission P_{st} at PCC is generally far below unity for grid connected wind farms. The following simple formula for $Coef(S_0, f_0, S_2, r)$ can be used provided 8 % uncertainty in P_{st} is allowable:

$$\begin{aligned} Coef(S_0, f_0, S_2, r) &\approx \frac{1}{36} S_0\, f_0{}^{1{,}55} + 10{,}14\, S_2 \\ &+ 0.1332\ Cosh\left[0{,}04462(r - 5{,}383)(r + 12{,}548)\right] \end{aligned} \qquad (40)$$

Recall that an imprecise PSD parameterization can introduce comparable uncertainties in P_{st}. The parameters have been estimated from PSD since PSD has superior stochastic properties than amplitude density spectrum. However, if the quantities are estimated from amplitude density spectrum, then the corresponding magnitudes are:

$$\left\langle S_{farm}(f) \right\rangle \approx S_1{}' \left(S_0{}'\, \delta_0(f - f_0{}') + f^{-r'} + S_2{}' \right) \qquad (41)$$

with $S_1 \approx \frac{2}{\pi} S_1{}'^2$, $S_0 \approx \frac{2}{\pi} S_0{}'^2$, $S_2 \approx \frac{2}{\pi} S_2{}'^2$, $r' \approx r$ and $f_0 \approx f_0{}'$ (the factor $2/\pi$ is the ratio of the mean squared to the second central moment of a Rayleigh random variable).

A. Flicker coefficients of standard IEC 61400-21

Standard IEC 61400-21 [16] states flicker emission assuming flicker is inversely proportional to $S_{k,fic}$ and it evaluates separate flicker contribution of continuous operation (mainly due to tower shadow and wind variability) and contribution of switching events (such as connection and disconnection of turbines and other components).

The flicker coefficient for continuous operation of a turbine defined in Standard IEC 61400-21 [16], $c(\psi_k)$, is the normalized short term flicker for 10 minutes measuring interval and $S_{k,fic} = 1\,p.u.$ For a wind farm, $c(\psi_k)$ is the flicker that the farm would emit if it is connected at a PCC with short-circuit impedance angle ψ and short-circuit power equal to the nominal power of the farm, $N\, S_n$.

$$\begin{aligned} c(\psi_k) &= P_{st} \frac{S_{k,fic}}{N\, S_n} = \\ &= \left[\cos(\psi_k) + \sin(\psi_k)\tan(\varphi)\right] \sqrt{\frac{S_1}{N S_n^2} Coef(S_0, f_0, S_2, r)} \end{aligned} \qquad (42)$$

where S_n is the nominal power of the turbine and N is the number of equivalent turbines in the wind farm. Notice also if $c(\psi_k)$ is given for some ψ_k and φ, the flicker for other operational conditions can be computed.

The flicker coefficient for continuous operation and annual average wind speed v_a, $c(\psi_k, v_a)$, is the averaged 99th percentile of $c(\psi_k)$ assuming Rayleigh distribution of wind. Since parameters r, S_0, f_0, S_1 and S_2 depend on wind regime, it is necessary to characterize the PSD for various wind speeds.

B. Flicker emission from several wind farms

At medium voltage and high voltage, the capacity of the grid to be perturbed is shared among generators and loads, and IEC 1000-3-7 [17] asses this capacity. Tower shadow, wind turbulence and generator/converter oscillations can be considered statistically independent continuous processes.

Since the first three blocks are almost lineal and PSD has circular symmetry, the output of the weighting filter $b(t)$ is linearly related to power fluctuations. The output of the squaring block 4a is $c(t) = b^2(t) \sim Gamma\left[\frac{1}{2}, 2\sigma_b{}^2\right]$, where $\sigma_b{}^2$ is computed from (4) and (23):

$$\mu_{flick}|_{overall} = \sigma_b{}^2 = \int_{0,05\ \mathrm{Hz}}^{35\ \mathrm{Hz}} \sum_{m=1}^{M\ farms} \sigma_b^2|_{farm\ m}(f)\, df \qquad (43)$$

where $\sigma_b^2|_{farm\ m}(f)$ is the variance of the phasor of the weighting filter output at frequency f and at farm number m. Since integration is a linear operation and summation and integration order can be interchanged, $\sigma_b{}^2$ can be computed separately for each wind farm and then just add the contributions up:

$$\mu_{flick}|_{overall} = \sum_{m=1}^{M\ farms} \sigma_b^2|_{farm\ m} = \sum_{m=1}^{M\ farms} \mu_{flick}|_{farm\ m} \qquad (44)$$

Since P_{st} is approximately proportional to $\sqrt{\mu_{flick}}$, then the quadratic law is suitable to estimate overall effect of several wind farms at a point of the grid.

$$P_{st}|_{overall} \approx 0,75\sqrt{\mu_{flick}} \approx \sqrt{\sum_{m=1}^{M\ farms} P_{st}^2|_{farm\ m}} \qquad (45)$$

Therefore, (38) and (45) indicate (in accordance to the central limit theorem) that quadratic law summation of the influence of each wind farm is more suitable during continuous operation than the default cubic summation suggested in IEC 1000-3-7 for unspecified cases.

The authors of this article performed several test in various wind farms with a conventional flickermeter and the influence of nearby loads masked the influence of the farms [9]. Thus, only measures adapted from IEC 61400-21 can estimate flicker emission from wind farms. The contribution of nearby wind farms to measured flicker is difficult to assess in actual measures since other flicker sources are predominant.

IV. Validation of the Model with Real Data

The instantaneous current and voltage have been measured at several wind farms and the flicker emission has been computed in the frequency domain to check the proposed model. Since data was available, P_{st} has been computed from actual PSD instead of using the adjusted parameters of the PSD.

P_{st} is almost proportional to the square root of the instantaneous flicker level average μ_{flick}, which can be computed from (20). The contribution of cross terms involved in the standard deviation of instantaneous flicker level σ_{flick} can be neglected in the first instance.

For the fixed speed, stall regulated turbine the principal contribution to flicker is due to tower shadow (rotor and blade frequencies). The contribution of frequencies 5-7,5 Hz is about ¼ of tower shadow in Fig 7.

In the 600 kW Vestas Opti-Slip turbine (variable resistor induction generator with pitch control), the influence of tower shadow (rotor and blade frequencies) is negligible. The flicker levels in Fig. 8 are the lowest of the measured turbines and its due mainly to frequency range 4-12 Hz.

In the doubly fed induction generator, pitch regulated turbine, the influence of tower shadow (rotor and blade frequencies) is small. The flicker is due mainly to frequencies 4-14 Hz in Fig 9.

Remolinos wind farm shows a similar behaviour than the single turbine. The value of μ_{flick} for the wind farm is approximately the value of measured wind turbine times the number of turbines in the wind farm (18). Since P_{st} approximately is proportional to the square root of μ_{flick}, the flicker emission of the wind farm can be computed from a single turbines: $P_{st}{}_{\text{wind farm}} \approx \sqrt{N} P_{st}{}_{\text{wind turbine}}$.

V. Conclusions

Power fluctuations in a wind farm depend on relative blade positions of the turbines and wind turbulence. The rotor can have any angle with approximately the same probability. Turbulence in the range of 0,05 Hz to power supply frequency are mainly uncorrelated for the usual distances in a wind farm. Thus, the overall behavior of a large number of wind turbines can be derived from the operation of a single turbine. The periodogram (module averaged Power Spectrum Density) has proved suitable to model wind power variability.

In induction generators analyzed with squirrel cage or variable resistance rotor, the turbine coupling is soft enough to damper high frequency oscillations and tower shadow and hence, wind turbulence is the main flicker source. In some doubly fed induction generators analyzed, the power converter control induces noise at frequencies around maximum flicker sensitivity and hence, this is the main flicker source. In all cases analyzed the flicker level was low due to the strength of the grit at PCC.

The results have been compared with experimental data through PSD (averaged spectrum periodograms) and spectograms (joint time-frequency domain).

VI. Acknoledgements

This work has been partially supported by Department of Education and Culture of Aragón (B134/1998 grant), Compañía Eólica Aragonesa S.A. (CEASA) and TAIM-NEG-MICON (now Vestas).

VII. ANNEX: PSD OF $b(t)$ AT SOME LOCATIONS

In the following graphs, the blue lines are the PSD of $b(t)$ and the red line is the area beneath the PSD from the left, $\sigma_b{}^2|_{f_{\max}} = \int_{0{,}05\,\mathrm{Hz}}^{f_{\max}} \sigma_b{}^2(f)\,df$, which equates μ_{flick} at $f_{\max} = 35\,\mathrm{Hz}$. The frequencies that contribute more to flicker are where red line steps up.

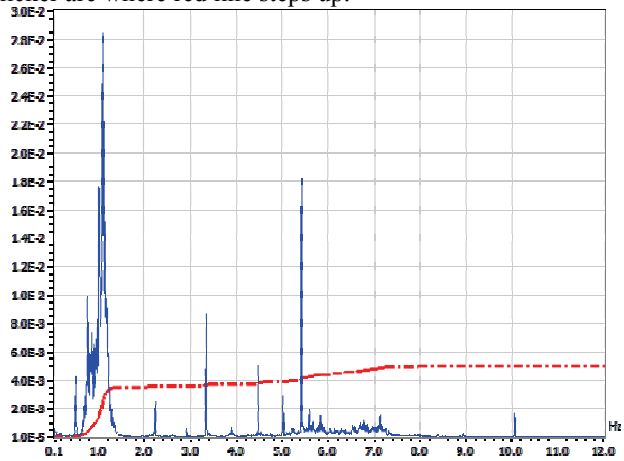

Fig. 6: PSD of squared voltage variations $b(t)$ and $\sigma_b{}^2|_{f_{\max}}$ for a SQIG (fixed speed, stall regulated) wind turbine and $\beta = 10^{-3}$.

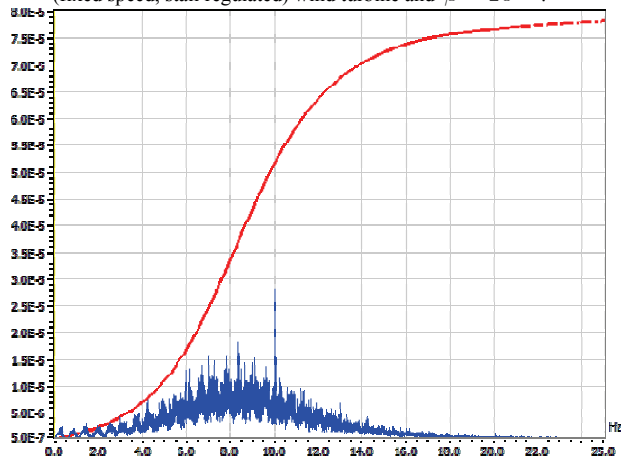

Fig. 7: PSD of squared voltage variations $b(t)$ and $\sigma_b{}^2|_{f_{\max}}$ for a VRIG (opti-slip) wind turbine and $\beta = 10^{-3}$.

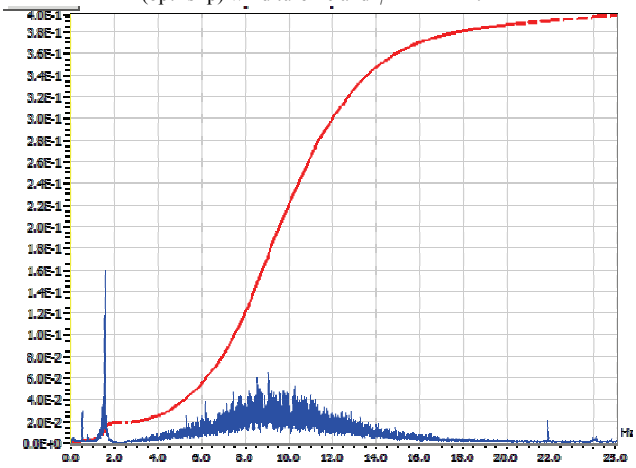

Fig. 8: PSD of squared voltage variations $b(t)$ and $\sigma_b{}^2|_{f_{\max}}$ for Remolinos wind farm and $\beta = 10^{-3}$.

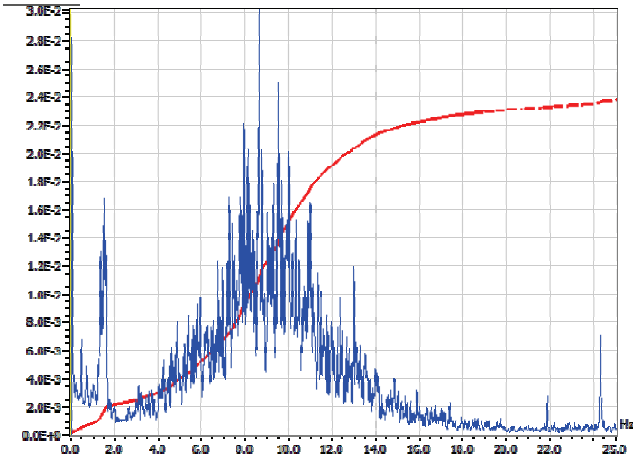

Fig. 9: PSD of squared voltage variations $b(t)$ and $\sigma_b{}^2|_{f_{\max}}$ for a DFIG (variable speed) wind turbine and $\beta = 10^{-3}$.

REFERENCES

[1] J. Mur, A.A. Bayod, "Characterization of Spectral Density of Wind Farm Power Output", EPQU 2007, Barcelona.

[2] P. Sorensen, N.A. Cutululis, A. Viguers-Rodriguez, L. E. Jensen, M.H. Donovan and H. Madsen, "Power Fluctuations From Large Wind Farms", IEEE Trans. On Power Systems, Vol. 22, No. 3, Aug. 2007.

[3] J. Mur, A.A. Bayod, "Pace of Tower Shadow Fluctuations in a Wind Farm", EPQU 2007, Barcelona. Available at: www.joaquinmur.eu

[4]Cristian Nichita, Dragos Luca, Brayima Dakyo, and Emil Ceanga, "Large Band Simulation of the Wind Speed for Real Time Wind Turbine Simulators", IEEE Transactions On Energy Conversion, Vol. 17, No. 4, December 2002.

[5]T. Petru and T. Thiringer, "Modeling of Wind Turbines for Power System Studies", IEEE Trans. On Power Systems, Vol. 17, No. 4, Nov. 2002, pp. 1132 - 1139

[6] E. Welfonder, R. Neifer and M. Spaimer, "Development And Experimental Identification Of Dynamic Models For Wind Turbines", Control Eng. Practice, Vol. 5, No. 1, pp. 63-73, 1997.

[7]P. Rosas, "Dynamic influences of wind power on the power system", Ph. D Thesis, Ørsted•DTU, March 2003, ISBN: 87-91184-16-9. Avalilable at www.risoe.dk/rispubl/ VEA/veapdf/ris-r-1408.pdf

[8] W. Schlez, D. Infield, "Horizontal, two point coherence for separations greater than the measurement height", Boundary-Layer Meteor. 87 (1998), 459-480.

[9] J. Mur, A.A. Bayod, S. Ortiz, R. Zapata, "Power Quality Analysis of Wind Turbines. Part II – Dynamic Analysis", ICREP 2003, Vigo.

[10] J. Cidrás, A.E. Feijóo, C. Carrillo González, "Synchronization of Asynchronous Wind Turbines" IEEE Trans, on Energy Conv., Vol. 17, No 4, Nov. 2002, pp 1162-1169

[11] C. Gherasim, "Signal Processing for Voltage and Current Measurements in Power Quality Assessment", PhD. Thesis, Katholieke Universiteit Leuven, May 2006

[12] J. Mur, J. Sallán, A.A. Bayod, "Statistical model of wind farms for power flow", ICREP 2003, Vigo.

[13] IEC 61400-4-15, Electromagnetic compatibility (EMC). Part 4: Testing and measurement techniques. Section 15: Flickermeter. Functional and design specifications.

[14] B. Picinbono, "On Circularity", IEEE Trans. On Signal Processing, Vol. 42, No 12, Dec. 1994., pp. 3473-3482

[15] J. Salo, H. M. El-Sallabi, and P. Vainikainen, "The Distribution of the Product of Independent Rayleigh Random Variables", IEEE Transactions On Antennas And Propagation, Vol. 54, No. 2, February 2006.

[16] IEC61400-21, Wind Turbine Generator Systems–Part 21: Measurement and assessment of power quality characteristics of grid connected wind turbines, IEC61400-21.

[17] CEI IEC 1000-3-7, Electromagnetic compatibility (EMC). Part 3: Limits – Section 7: Assessment of emission limits for fluctuating loads in MV and HV power systems – Basic EMC publication.